SLAC-PUB-10773
BABAR-TALK-04/094
hep-ex/0409068
September 2004

Selected Topics in *CP* Violation and Weak Decays from *BABAR**

J.J.Back
Department of Physics, University of Warwick,
Coventry, CV4 7AL, UK
(for the *BABAR* Collaboration)

Abstract

We present branching fraction and *CP* asymmetry results for a variety of charmless B decays based on up to 124 fb^{-1} collected by the *BABAR* experiment running near the $\Upsilon(4S)$ resonance at the PEP-II e^+e^- B-factory.

Presented at QCD 04: High Energy Physics International Conference
in Quantum Chromodynamics, Montpellier, France, 5-9 July 2004.
Submitted to Nuclear Physics B (Proceedings Supplement).

Stanford Linear Accelerator Center, Stanford University, Stanford, CA 94309

*Work supported in part by Department of Energy contract DE-AC02-76SF00515.

1 Introduction

CP violation has been established in the B-meson system [1] [2] and B-factories are now focusing their attention on over-constraining the angles and sides of the Unitarity Triangle, which is a partial representation of the Cabibbo-Kobayashi-Maskawa (CKM) matrix [3]. The study of charmless B decays allows us to make such measurements and also to probe physics beyond the Standard Model (SM). In this paper, we present the preliminary results of a few charmless analyses.

2 *CP* Asymmetries in B Decays

For charged B decays, *CP* violation can occur when we have at least two interfering amplitudes that have different weak and strong phases. This is known as direct *CP* violation, and manifests itself as an asymmetry in the partial decay rates for particle and anti-particle:

$$\mathcal{A}_{\rm direct} = \frac{\Gamma(B^- \to f^-) - \Gamma(B^+ \to f^+)}{\Gamma(B^- \to f^-) + \Gamma(B^+ \to f^+)} \tag{1}$$

where $\Gamma(B^- \to f^-)$ is the decay rate for $B^- \to f^-$, and $\Gamma(B^+ \to f^+)$ is the decay rate for the charge-conjugate process.

For neutral B decays, *CP* violation is present when we have interference between B^0 and $\bar{B}^0$ decays, with and without mixing, and manifests itself as a difference in the decay rates of the B mesons to a common final state. The asymmetric beam configuration of the *BABAR* experiment provides a boost of $\beta\gamma = 0.56$ to the $\Upsilon(4S)$ in the laboratory frame, which allows the measurement of the decay time difference Δt between the B^0 and $\bar{B}^0$ mesons along the beam axis. We fully reconstruct the signal B decay and partially reconstruct the other B meson in order to determine its flavour, i.e. whether it is B^0 or $\bar{B}^0$. We can then measure the *CP*-violating parameters C and S by fitting the following function to the decay time distribution (taking into account experimental resolution effects):

$$f(\Delta t) \;=\; \frac{e^{-|\Delta t|/\tau}}{4\tau}[1 + Q_{\rm tag} S \sin(\Delta m_d \Delta t) - Q_{\rm tag} C \cos(\Delta m_d \Delta t)], \tag{2}$$

where $Q_{\rm tag} = 1(-1)$ when the tagging meson is a B^0 ($\bar{B}^0$), τ is the mean B^0 lifetime, and Δm_d is the B^0-$\bar{B}^0$ oscillation frequency corresponding to the mass difference between the two mesons. The presence of mixing-induced *CP* violation would give a non-zero value for S, while direct *CP* violation would be indicated by a non-zero value of C.

3 The *BABAR* Detector

The results presented in this paper are based on an integrated luminosity of up to 124 fb^{-1} collected at the $\Upsilon(4S)$ resonance with the *BABAR* detector [4] at the PEP-II asymmetric e^+e^- collider at the Stanford Linear Accelerator Center. Charged particle track parameters are measured by a five-layer double-sided silicon vertex tracker and a 40-layer drift chamber located in a 1.5-T magnetic field. Charged particle identification is achieved with an internally reflecting ring imaging Cherenkov detector and from the average dE/dx energy loss measured in the tracking devices. Photons and neutral pions (π^0s) are detected with an electromagnetic calorimeter (EMC) consisting of 6580 CsI(Tl) crystals. An instrumented flux return (IFR), containing multiple layers of resistive plate chambers, provides muon and long-lived hadron identification.

4 B Decay Reconstruction

The B meson candidates are identified kinematically using two independent variables. The first is $\Delta E = E^* - E^*_{beam}$, which is peaked at zero for signal events, since the energy of the B candidate in the $\Upsilon(4S)$ rest frame, E^*, must be equal to the energy of the beam, E^*_{beam}, by energy conservation. The second is the beam-energy substituted mass, $m_{\rm ES} = \sqrt{(E^{*2}_{beam} - \mathbf{p}^{*2}_B)}$, where $\mathbf{p}^*_B$ is the momentum of the B meson in the $\Upsilon(4S)$ rest frame, and must be close to the nominal B mass [5]. The resolution of $m_{\rm ES}$ is dominated by the beam energy spread and is approximately 2.5 MeV/c^2. Figure 1 shows an example $m_{\rm ES}$ distribution.

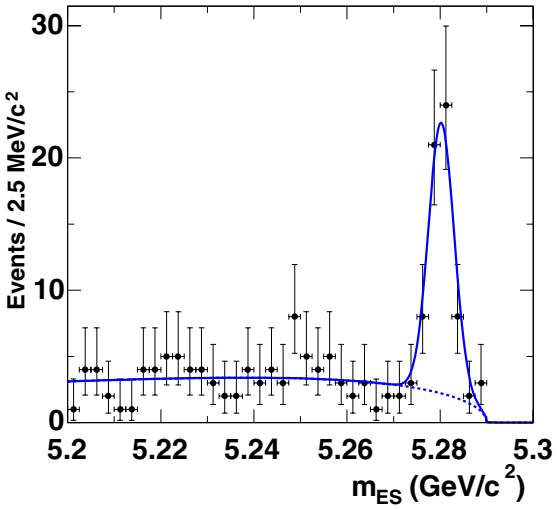

Figure 1: Distribution of the $m_{\rm ES}$ variable for $B^0 \to \phi K^{*0}$ decays. The solid line represents the fit to all of the data, while the dotted line shows the background contribution.

Several of the B modes presented here have decays that involve K^0_S and π^0 particles. K^0_S candidates are made by combining oppositely charged pions with requirements made on the invariant mass (to be, typically, within 15 MeV/c^2 of the nominal mass [5]), the flight direction and decay vertex. Neutral pion candidates are formed by combining pairs of photons in the EMC, with requirements made on the energies of the photons and the mass and energy of the π^0.

Significant backgrounds from light quark-antiquark continuum events are suppressed using various event shape variables which exploit the difference in the event topologies in the centre-of-mass frame between background events, which have a di-jet structure, and signal events, which tend to be rather spherical. One example is the cosine of the angle θ^*_T between the thrust axis of the signal B candidate and the thrust axis of the rest of the tracks and neutrals in the event. This variable is strongly peaked at unity for continuum backgrounds and has a flat distribution for signal.

Further suppression of backgrounds can be achieved using a Fisher discriminant, which is a linear combination of event shape variables, such as the Legendre moments $L_j = \sum_i p_i \times |\cos\theta_i|^{\rm j}$, where θ_i is the angle with respect to the B thrust axis of the track or neutral cluster i, p_i is its momentum, and the sum excludes the signal B candidate. The coefficients of the Fisher discriminant are chosen such that the separation between signal and background is maximised.

Sidebands in on-resonance ($\Upsilon(4S)$) data are used to characterise the light quark background in

ΔE and $m_{\rm ES}$, as well as data taken at 40 MeV below the $\Upsilon(4S)$ resonance ("off-resonance"). The phenomenologically motivated Argus function [6] is used to fit the background $m_{\rm ES}$ distributions. Control samples are used to compare the performance between Monte Carlo simulated events and on-resonance data.

All of the analyses have been performed "blind", meaning that the signal region is looked at only after the selection criteria have been finalised (in order to reduce the risk of bias). Charge conjugate modes are implied throughout this paper.

5 $b \to s\bar{s}s$ Gluonic Penguin Modes

Here we describe the *CP* violation results of the B-decay modes ϕK^0, $K^+K^-K^0_S$, $KK^0_SK^0_S$ and $f_0(980)K^0_S$, which are dominated by penguin-type Feynman diagrams. Neglecting CKM-suppressed amplitudes, these decays have the same weak phase as the decay $B^0 \to J/\psi K^0$ [7]. However, the presence of heavy particles in the penguin loops may give rise to other *CP*-violating phases. It is therefore important to measure *CP* violation in these modes and compare with the SM predictions to test whether there is physics beyond the SM. The measured branching fractions and *CP*-asymmetry parameters are shown in Table 1.

Table 1: Measurements of the branching fractions ($\mathcal{B}$) and *CP*-asymmetry parameters for various gluonic $b \to s\bar{s}s$ penguin modes. Results in square brackets denote limits at the 90% confidence level. The first and second uncertainties show the statistical and systematic errors, respectively. The third error for the branching fraction of $f_0(980)K^0_S$ represents model-dependent uncertainties.

Mode	$\mathcal{B}(\times 10^{-6})$	S	C	$\mathcal{A}_{\rm direct}$
ϕK^0	—	$0.47 \pm 0.34^{+0.08}_{-0.06}$	$0.01 \pm 0.33 \pm 0.10$	—
ϕK^0_S	—	0.45 ± 0.43	-0.38 ± 0.37	—
$K^+K^-K^0_S$	$(23.8 \pm 2.0 \pm 1.6)$	$-0.56 \pm 0.25 \pm 0.04$	$-0.10 \pm 0.19 \pm 0.09$	—
$K^+K^0_SK^0_S$	$(10.7 \pm 1.2 \pm 1.0)$	—	—	$-0.04 \pm 0.11 \pm 0.02$ $[-0.23, 0.15]$
$f_0(980)K^0_S$	$(6.0 \pm 0.9 \pm 0.6 \pm 1.2)$	$-1.62^{+0.56}_{-0.15} \pm 0.10$	$0.27 \pm 0.36 \pm 0.12$	—

5.1 $B^0 \to \phi K^0$

The mode $B \to \phi K^0$ is reconstructed using both K^0_S and K^0_L decays, with $\phi \to K^+K^-$ and $K^0_S \to \pi^+\pi^-$. The two-kaon invariant mass is required to be within 16 MeV/c^2 of the nominal ϕ mass [5], while K^0_L candidates are identified using information from the EMC and IFR. To validate the analysis, the control sample $B^\pm \to \phi K^\pm$ is used, in which the measured *CP*-asymmetry parameters are $S = 0.23 \pm 0.24$ and $C = -0.14 \pm 0.18$, which are consistent with the SM expectation of no *CP* violation. The results for this mode presented in Table 1 are consistent with the SM. Figure 2 shows the decay time distributions for this mode.

5.2 $B^0 \to K^+K^-K^0_S$

The decay $B^0 \to K^+K^-K^0_S$ has the same final state as the previous mode, except that events containing the $\phi \to K^+K^-$ resonance are removed. This sample is several times larger than the sample of ϕK^0_S, and therefore provides a more accurate way to measure the *CP*-violating parameters for this final state. The measured *CP*-even fraction of this decay, equal to $2\Gamma(B^+ \to$

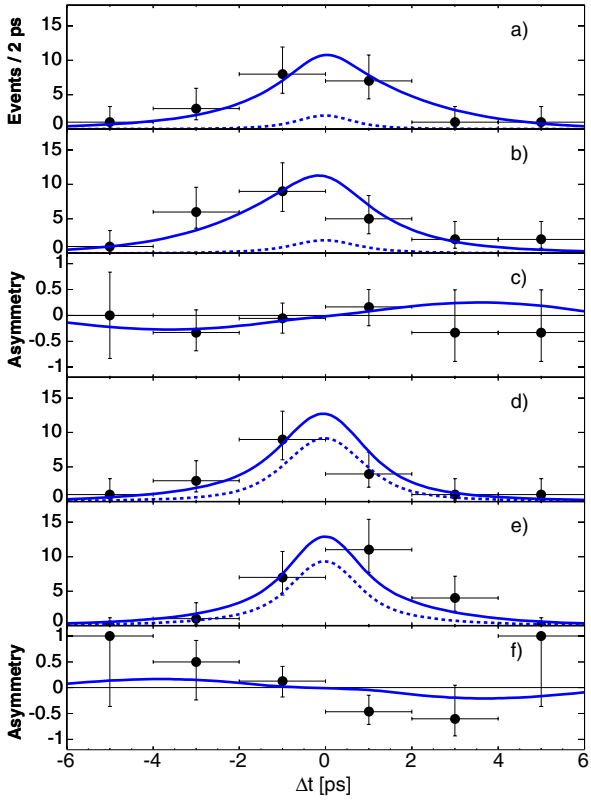

Figure 2: Plots of the Δt distributions, for (a) B^0- and (b) $\bar{B}^0$-tagged ϕK^0_S events, with plot c) showing the asymmetry. Plots d), e) and f) show the corresponding plots for ϕK^0_L candidates.

$K^+K^0_SK^0_S)/\Gamma(B^0 \to K^+K^-K^0)$, is $0.98 \pm 0.15 \pm 0.04$. This implies that the final state is *CP*-even dominated. The values of S and C shown in Table 1 are consistent with the SM, and setting C to zero gives a value of sin2β of $0.57 \pm 0.26 \pm 0.04^{+0.17}_{-0.00}$, where the last error represents the uncertainty on the *CP* content. This result is consistent with the world-average value of 0.73 ± 0.05 [5].

5.3 $B^+ \to K^+K^0_SK^0_S$

In the SM, we expect that the decay rates for $B^+ \to K^+K^0_SK^0_S$ and $B^- \to K^-K^0_SK^0_S$ to be equal, although contributions from physics beyond the SM could give a non-zero direct *CP* asymmetry. We measure an asymmetry that is consistent with zero, as shown in Table 1.

5.4 $B^0 \to f_0(980)K^0_S$

This mode is reconstructed with the decays $f_0(980) \to \pi^+\pi^-$ and $K^0_S \to \pi^+\pi^-$. The invariant mass of the $f_0(980)$ resonance is required to be between 0.86 and 1.10 GeV/c^2, and is parameterised as a relativistic Breit-Wigner, with a measured mass of $(980.6 \pm 4.1 \pm 0.5 \pm 4.0)$ MeV/c^2 and width of $(43^{+12}_{-9} \pm 3 \pm 9)$ MeV/c^2, where the last errors are uncertainties due to interference effects from other resonances in the $B^0 \to K^0_S\pi^+\pi^-$ Dalitz plot. These values are in agreement with previous measurements [5]. The results of S and C for this mode (see Table 1) are consistent with the SM

at the 1.7σ and 0.8σ levels, respectively.

6 $B^0 \to \rho^+\rho^-$

The time-dependent *CP*-violating asymmetry in the decay $B^0 \to \rho^+\rho^-$ is related to the CKM angle α. If the decay proceeds only through tree diagrams, then the asymmetry is directly related to α. However, we can only measure an effective angle, $\alpha_{\rm eff}$, if there is pollution from gluonic penguins. Recent measurements of the $B^+ \to \rho^+\rho^0$ branching fraction and upper limit for $B^0 \to \rho^0\rho^0$ [8] indicate that the penguin pollution is small, which has been argued theoretically [9]. It has also been found that the longitudinal polarisation dominates this decay [10], which simplifies the *CP* analysis.

The ρ candidates are required to have an invariant mass between 0.5 and 1.0 GeV/c^2, and combinatorial backgrounds are suppressed by applying selection criteria to several event shape variables. An unbinned maximum likelihood fit is performed to extract the following preliminary *CP*-asymmetry results, assuming that the decay has zero transverse polarisation: $S_{\rm long} = -0.19 \pm 0.33 \pm 0.11$ and $C_{\rm long} = -0.23 \pm 0.24 \pm 0.14$, where the first errors are statistical and the second errors are systematic uncertainties. The branching fraction for this mode is measured to be $(30 \pm 4 \pm 5) \times 10^{-6}$.

The CKM angle α can be constrained by performing an isospin analysis of $B \to \rho\rho$ [11], which needs as input the amplitudes of the *CP*-even longitidunal polarisation of the B meson decaying into $\rho^\pm\rho^0$, $\rho^0\rho^0$ and $\rho^+\rho^-$, and the measured values of $S_{\rm long}$ and $C_{\rm long}$ given above. Assuming that isospin symmetry is valid, and that there are no significant non-resonant or $I = 1$ isospin contributions, the best CKM fit to the data gives the preliminary result of $\alpha = (96 \pm 10 \pm 4 \pm 13)^\circ$, where the last error is the uncertainty from possible penguin pollution, which is estimated by using the measured Grossman-Quinn bound [11]: $|\alpha_{\rm eff} - \alpha| < 13^\circ (15.9^\circ)$ at 68.3% (90%) C.L. Figure 3 shows the value of α as a function of the confidence level.

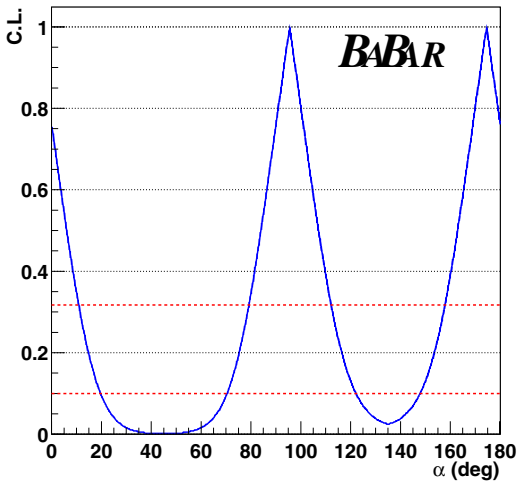

Figure 3: The value of α as a function of confidence level from the preliminary results of the isospin analysis of $B \to \rho\rho$. The dotted red lines represent the 10% and 31.7% confidence levels.

7 $B^0 \to \phi K^{*0}(892)$

This mode is dominated by $b \to s\bar{s}s$ penguin diagrams, like the modes presented in Sec. 5, and angular correlation measurements and *CP*-asymmetries are sensitive to contributions beyond the SM.

The decay rate of this channel depends on the helicity amplitudes A_λ of the vector mesons, where $\lambda = 0$ or ± 1 [12]. These amplitudes can be expressed in terms of their *CP*-even and *CP*-odd equivalents: $A_{||} = (A_{+1} + A_{-1})/\sqrt{2}$ and $A_\perp = (A_{+1} - A_{-1})/\sqrt{2}$. From this, it follows that the longitudinal and transverse fractions are $f_L = |A_0|^2/\sum|A_\lambda|^2$ and $f_\perp = |A_\perp|^2/\sum|A_\lambda|^2$, respectively. The relative phases of the *CP*-even and *CP*-odd amplitudes are $\phi_{||} = \arg(A_{||}/A_0)$ and $\phi_\perp = \arg(A_\perp/A_0)$, respectively. From the above, one can derive the vector triple-product asymmetries $\mathcal{A}_T^{||}$ and $\mathcal{A}_T^0$, which are sensitive to *CP*-violation [13]:

$$\mathcal{A}_T^{||,0} = \frac{1}{2}\left(\frac{\mathrm{Im}(A_\perp A^*_{||,0})}{\sum|A_\lambda|^2} + \frac{\mathrm{Im}(\bar{A}_\perp \bar{A}^*_{||,0})}{\sum|\bar{A}_\lambda|^2}\right), \tag{3}$$

where $\bar{A}_\lambda$ represents the conjugate helicity amplitude.

B mesons are reconstructed by combining $\phi \to K^+K^-$ and $K^{*0} \to K^+\pi^-$ candidates. The invariant masses of the ϕ and K^{*0} are required to be between 0.99 and 1.05 GeV/c^2, and between 1.13 and 1.73 GeV/c^2, respectively. Continuum backgrounds are suppressed by using event shape variables.

Table 2 shows the preliminary results for this mode, using an unbinned maximum likelihood fit to the data. We observe non-zero contributions from all three helicity amplitudes $|A_0|$, $|A_{||}|$ and $|A_\perp|$, with more than 5σ significance, as shown in Fig. 4. The longitudinal polarisation is essentially a factor of two less than that for $B \to \rho\rho$ [10], which could be a hint of physics beyond the SM. However, this difference may be related to long-distance effects from $c\bar{c}$ penguins [14]. There is no evidence for direct *CP* violation.

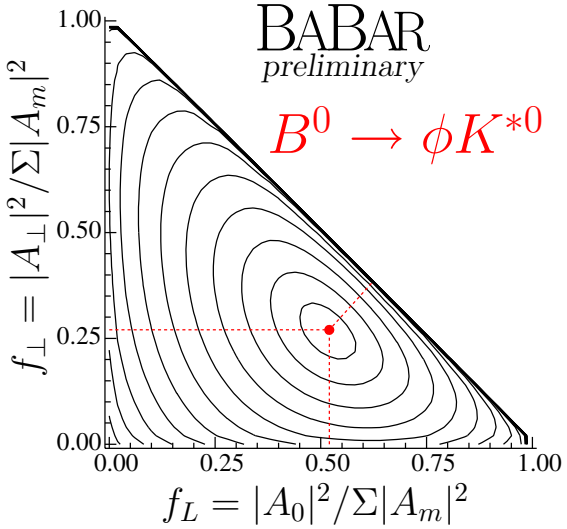

Figure 4: Plot of transverse (*CP*-odd) versus longitudinal polarisation for $B^0 \to \phi K^{*0}$, showing likelihood function contours with 1σ intervals. The dot represents the fit result.

Table 2: Preliminary results of the angular analysis of the decay $B^0 \to \phi K^{*0}$. $\mathcal{B}$ denotes the branching fraction, while $\mathcal{A}_{CP}$, $\mathcal{A}^0_{CP}$ and $\mathcal{A}^\perp_{CP}$ denote the direct, longitudinal and transverse *CP*-asymmetries, respectively. The *CP*-even and *CP*-odd phase differences are given by $\Delta\phi_{||} = \frac{1}{2}(\phi^+_{||} - \phi^-_{||})$ and $\Delta\phi_\perp = \frac{1}{2}(\phi^+_\perp - \phi^-_\perp)$, respectively, while the triple product asymmetries are denoted by $\mathcal{A}^{||,0}_T$.

Variable	Result
$\mathcal{B}$	$(9.2 \pm 0.9 \pm 0.5) \times 10^{-6}$
f_L	$0.52 \pm 0.07 \pm 0.02$
$f_\perp$	$0.27 \pm 0.07 \pm 0.02$
$\phi_{||}$	$2.63^{+0.24}_{-0.23} \pm 0.04$
$\phi_\perp$	$2.71^{+0.22}_{-0.24} \pm 0.03$
$\mathcal{A}_{CP}$	$-0.12 \pm 0.10 \pm 0.03$
$\mathcal{A}^0_{CP}$	$-0.02 \pm 0.12 \pm 0.01$
$\mathcal{A}^\perp_{CP}$	$-0.10^{+0.25}_{-0.27} \pm 0.04$
$\Delta\phi_{||}$	$0.38^{+0.23}_{-0.22} \pm 0.03$
$\Delta\phi_\perp$	$0.30^{+0.24}_{-0.22} \pm 0.03$
$\mathcal{A}^{||}_T$	$0.02 \pm 0.05 \pm 0.01$
$\mathcal{A}^0_T$	$0.11 \pm 0.07 \pm 0.01$

8 Conclusions

We have shown a selection of results from the *BABAR* experiment based on up to 124 fb^{-1} collected at the $\Upsilon(4S)$ resonance. The SM is consistent with the measurements presented here, although there are hints of physics beyond the SM in $b \to s$ penguin modes. We can expect a more definite conclusion to this exciting prospect in the near future.

References

[1] *BABAR* Collaboration, B. Aubert *et al.,* Phys. Rev. Lett. **89**, 201802 (2002).

[2] BELLE Collaboration, K. Abe *et al.,* hep-ex/0308036.

[3] N. Cabibbo, Phys. Rev. Lett. **10**, 531 (1963); M. Kobayashi and T. Maskawa, Prog. Theor. Phys. **49**, 652 (1973).

[4] *BABAR* Collaboration, B. Aubert *et al.,* Nucl. Instr. and Meth. A **479**, 1 (2002).

[5] Particle Data Group, S. Eidelman *et al.,* Phys. Lett. B **592**, 1 (2004).

[6] ARGUS Collaboration, H. Albrecht *et al.,*Z. Phys. C **48**, 543 (1990).

[7] Y. Grossman and M. P. Worah, Phys. Lett. B **395**, 241 (1997); D. London and A. Soni, Phys. Lett. B **407**, 61 (1997).

[8] *BABAR* Collaboration, B. Aubert *et al.,* Phys. Rev. Lett. **91**, 171802 (2003); BELLE Collaboration, J. Zhang *et al.,* Phys. Rev. Lett. **91**, 221801 (2003); *BABAR* Collaboration, B. Aubert *et al.,* hep-ex/0408061.

[9] R. Aleksan *et al.,* Phys. Lett. B **356**, 95 (1995).

[10] *BABAR* Collaboration, B. Aubert *et al.,* Phys. Rev. D **69** 031102 (2004).

[11] M. Gronau, D. London, Phys. Rev. Lett. **65**, 3381 (1990); Y. Grossman and H. Quinn, Phys. Rev. D **58**, 017504 (1998).

[12] G. Kramer and W. F. Palmer, Phys. Rev. D **45**, 193 (1992).

[13] G. Valencia, Phys. Rev. D **39**, 3339 (1989).

[14] C. W. Bauer *et al.,* hep-ph/0401188 (2004).